EDELWEISS PUBLICATIONS
OPEN ACCESS

https://doi.org/10.33805/2690-2575.109
Volume 2 Issue 1 | PDF 109 | Pages 5

Nanomaterial Chemistry and Technology

Research Article ISSN 2690-2575

Preparation and Characterization of SnO_2 Nanoparticles for Antibacterial Properties

Bilal Ahmad Thoker[1]*, Asif Ahmad Bhat[1]*, Atif Khurshid wani[2], Masood Ayoub Kaloo[3]* and Gulzar Ahmad Shergojri[4]

Affiliation

[1]School of Physical Sciences, Lovely Professional University, Punjab, India
[2]School of Bioengineering and Biosciences, Lovely Professional University, India
[3]Department of Chemistry, Govt. Model Degree College Shopian, Jammu and Kashmir, India
[4]Department of Physics, Govt. Model Degree College Shopian, Jammu and Kashmir, India

***Corresponding author:** Masood Ayoub Kaloo, Department of Chemistry, Govt. Model Degree College Shopian-192303, Jammu and Kashmir, India, E-mail: kaloomasood@gmail.com

Citation: Thoker BA, Bhat AA, Wani AK, Kaloo MA and Shergojri GA. Preparation and characterization of SnO_2 nanoparticles for antibacterial properties (2020) Nanomaterial Chem Technol 2: 1-5.

Received: Sep 09, 2020
Accepted: Oct 26, 2020
Published: Nov 02, 2020

Abstract

To investigate morphological, optical and antibacterial properties of SnO_2 nanoparticles which are synthesized by using an easy and affordable Sol-Gel method. By using various techniques such as XRD (X-ray Powder Diffraction), FT-IR (Fourier Transform Infrared), UV-Vis, PL, SEM (Search Engine Marketing), EDAX (Energy Dispersive X-Ray Analysis), the structural, optical, composition of elements and the size of the SnO_2 nanoparticles (NPs) has been discussed. The variation in properties of SnO_2 as synthesized and at annealing temperatures has also been discussed. Size of tin oxide Nano particles from XRD is found in the range of 9-10 nm, and the lattice parameters about $a=b=4.7306^0A$, $c=3.69^0A$. From UV-Vis it is found that the band gap of tin oxide decreases as we increase the temperature. Active efficiency of SnO_2 NPs has been tested on Gram negative (*E.coli*) and gram positive (*Micrococcus luteus*) bacteria on the growth of pure culture using zone inhibition method.

Keywords: Tin Oxide, Gram positive, Gram negative, *E.coli*, *Micrococcus luteus*, Zone of inhibition.

Abbreviations: CVD-Chemical Vapor Deposition, FTIR-Fourier Transform Infrared, XRD-X-ray Powder Diffraction, SEM-Search Engine Marketing, EDAX-Energy Dispersive X-Ray Analysis.

Introduction

In recent years, tin oxide (SnO_2) has got lot of attention due to its numerous properties such as high transparency degree in visible spectrum. SnO_2 acts as an n-type semiconductor having a wide band gap of 3.6-3.8eV at 330K. These include transport conducting electrodes, Flat displays, super capacitors, rechargeable Li batteries, optical electronic devices, Microelectronic devices liquid crystal displays, solar cell electrodes, transistors, catalyst supports for oxidation of organic compounds. The secret behind these numerous application of Tin oxides due to its chemical and mechanical stability, A number of methods is used to prepare the Tin Oxides include Thermal evaporation of oxides, rapid oxidation of pure Tin, chemical vapor deposition CVD (Chemical Vapor Deposition), spray pyrolysis, evaporating Tin grains in air. SnO_2 is having the cassiterite structure [1-4].

At the center each Tin atom is surrounded by six Oxygen atoms which are nearly placed at the corners of the equilateral triangle. Thus the Structure is 6:3 co-ordination the lattice parameter are $a=4.737^0A$ and $c=3.185^0A$, the c/a ratio is 0.673, Hydrothermal method. To improve the properties of tin oxide such as structural, electrical and also the optical properties of the synthesized SnO_2, many researchers has study the effect of the temperature, doping concentration, deposition rate, substrates, oxygen partial pressure and the annealing temperatures were widely executed. The annealing temperature processes can be used in the reduction of the intrinsic stress, and to improve the lattice miss-alignment or mismatch and to create longer mean paths for the mobile electrons due to thermal vibrations in getting better electrical conductivity [3,5,6].

In this work, The Sol-Gel method is used to synthesize the SnO_2 nanoparticles. In order to study the characterization of materials for structural, morphological and optical properties and composition, various techniques such as XRD, FT-IR, UV-Vis, TEM, SEM, and PL were used. Once the characterization was done, study regarding the antibacterial properties on two bacteria's E. coli (generally gram negative) and *Micrococcus lettuces* (Gram positive) of the Tin Oxide was studied.

Experimental

Tin (II) Chloride or Stannous Chloride ($SnCl_2.2H_2O$) (99%.CDH, M.W 225.64), Ammonia (NH_3) (99%, M.W 17.03), ethanol (25%, DI water, nutrient Agar granulated (95%, Himedia), Agar Agar type 1 (95%, Himedia, M.W 336.34), Analytical, M.W 46.07), Acetone (M.W 58.08), Pure culture bacteria (100%, Himedia).

Synthesis of Tin Oxide nanoparticles By Sol-gel Method

Take 11.2815 gm of pure Stannous Chloride (0.5M) put in a beaker containing 100 ml distilled water. Stirrer it well for 10 minutes on the magnetic stirrer and keep the temperature 85^{0}C. Then mix 5 ML of ammonia to the beaker and stir the solution for 10 minutes. Leave the solution as such for salting and cover the beaker with the aluminum foil so that no impurity will add in the solution. After 3 hours remove the extra water, then again put the distilled water and again keep the solution for salting. Repeat the same procedure for 4-5 times. Wash the solution with ethanol by 2 times, after that filter the solution. Then put the filtrate in the cru-sever china dish or glass plate. Then take the different solution to keep at 200, 300, 400, and 500^{0}C for 2 hours with the help of a Muffle Furnace (MSW-101).

Preparation of Nutrient Agar Solution

First of all pour 150ml of Distilled water in a cylindrical flask. Add 4.2gm of nutrient agar solution into it then stir it gently if the solution is dissolved then use the cotton to pluck the flask otherwise add 3gm of Agar-Agar solution then again stir the solution then pluck the solution tightly. By placing the cylindrical flask in an autoclave for 1 hour under the parameters of 121^{0}C temperature and 15 atm pressure. After 1 hour release the pressure slowly to 0. Before getting solidifies the solution we have to pour the nutrient solution into different Petri plates (All task in done in the laminar). Keep the Petri dishes as such for at least 15 minutes under the UV light of the laminar. Hence our nutrient agar solution has been prepared.

Preparation of *E Coli* and *Micrococcus Lutes*

We have taken the ampoules present in powder form (nutrient broth). Here 0.78 grams dissolved in 60ml water were put in test tube. Test tubes were placed in autoclave for one hour followed by inoculation (addition of pure culture). Then pure culture was put in a test tube along with a control test tube. The test tubes were placed in an incubator for 24 hours at 37ºC. After 24 hours growth of strains was checked with control test tube.

Results and Discussions

Structural properties by XRD

By using the powder X-ray diffraction measurements (PAN analytical) using the Cu Kα having wavelength λ= 1.540598^{0}A as the incident radiation X-rays source to study the structural properties of SnO_2 Nano-particles operated at 30 kV and at 40 mA voltage and current respectively over the range 20º to 80º degrees. The graph is plotted between angle 2θ in degrees along X-axis and the intensity along Y-axis in the range 20º-80º and 0-4500 a.u respectively.

Using the Scherer formula for the SnO_2 Nano-powders we can calculate the d (hkl) the average crystalline size of the planes present in the SnO_2 Nano-powders.

$$D\,(hkl) = K\lambda/\beta\cos\theta$$

Where, K represents the shape factor which is usually taken as 0.9, λ is the wavelength of the X-rays used as the incident source, θ is the Braggs angle and β is known as the (FWHM) full width half maximum. The analysis of the SnO_2 Nano-particles is being done by the powder X-ray Diffractometry is used to identify the crystal structure, identify the phase and calculate the average size of the grain sample. The SnO_2 was synthesize by Sol-gel method and the XRD pattern of the SnO_2 as synthesized and at 500ºC were recorded in **Figure 1**.

From the XRD pattern it was found that the following crystals planes are present in the SnO2 (110), (101), (200), (211), (220), (002), (310), (112), (301), (202) and (321) were indicating that the SnO2 is polycrystalline in nature and having rutile tetragonal structure [JCPDS Card No; 41-1445] [7,13].

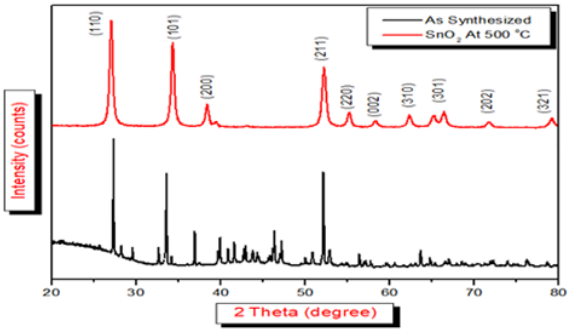

Figure 1: XRD plot of SnO_2 as Synthesized and at 500ºC.

S.No	(hkl)	2θ (degrees)	Intensity	d-spacing	FWHM
1	-110	26.6184	3010.322	3.344	0.6064
2	-101	33.9114	2462.958	2.6401	0.6214
3	-200	37.9914	711.462	2.3655	0.6278
4	-211	51.8124	1762.891	1.7631	0.5476
5	-220	54.7874	476.3504	1.6742	0.6165
6	-2	58.0004	242.4645	1.5889	0.4572
7	-310	61.9614	409.1954	1.4965	0.4432
8	-112	64.8004	395.4304	1.4376	0.4075
9	-310	65.8544	376.1922	1.4171	0.6573
10	-202	71.4474	212.6134	1.3193	0.6473
11	-321	78.7914	336.8293	1.2137	0.6032

Table 1: Showing different peaks having different intensities and having different d-spacing values and showing FWHM values.

By using the following formula, we can estimate the average value of the lattice constant for the different planes (hkl) present in the sample.

$$\mathbf{a = d/\sqrt{} + k^2 + l^2}$$

Where, α is the lattice constant, d is the inter-planer spacing and (hkl) are known as miller indices. The average calculated value for the lattice constant a=b=4.7306ºA and c=3.69ºA.

S.No	(hkl)	Lettice parameter a =b (nm)	Lattice parameter c (nm)	Size from Scerrer equation (nm)
1	-110	4.7303	3.2923	4.7306 ± 0.50
2	-101	4.4591	3.5946	4.7739 ± 0.50
3	-200	4.7851	3.6136	5.4613 ± 0.50
4	-211	4.6871	3.8274	4.9013 ± 0.50
5	-220	4.7303	3.2923	4.7306 ± 0.50

Table 2: Comparison of particle size, lattice parameters and the particle size from Scherer equation of different (hkl) planes.

Optical properties by UV-vis Spectroscopy

To study about the absorption of SnO_2 in UV-Vis spectrum we use the UV spectrometer and also study about the peak absorbance as well as the band gap of SnO_2 nanoparticles. And also study about the variation of energy band gap with increasing temperature. And discuss about the quantum confinement or quantum effect which has been shown by the SnO_2 [8,9,10,21].

In optical absorption, the Nano sized semiconductor exhibit generally threshold energy. This is due to the band gap structures. The decreasing size is due to the absorption of the blue shift (when the size of the SnO_2 nanoparticles approaches to the Bohr radius also called the quantum confinement is reflected at the edges of the structures. The above graph gives the information of the absorption by the Tin Oxide in the visible and ultra violet range. There is variation in the absorption with respect to the incident wavelength [21].

There is enhancement (increase) in absorption as the temperature increases with respect to the synthesized Tin Oxide. Therefore it shows the blue shift due to absorption in the UV-Vis region at the 259.20 nm. The peak value of absorption remains same for Tin oxide even after annealing at different temperatures **Figure 2** [7,11,12].

The energy band gap is calculated by the following relation

$$E_g = h*c/\lambda$$

Where, Eg is optical energy band gap, h is Planks constant, c is the speed of light, λ is the cut- off frequency [14,16].

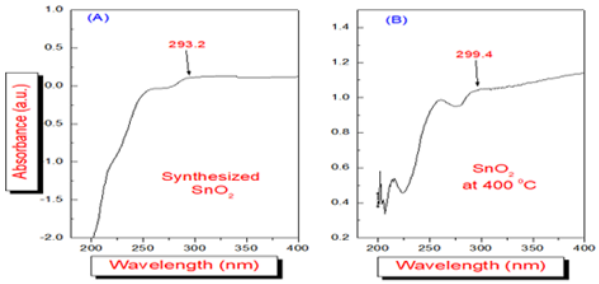

Figure 2: shows the cut-off frequency for Synthesized SnO_2 [Figure 2A and Figure 2B] and the cut-off frequency for SnO_2 at 400^{0}C [15].

Estimation of Band Gap of SnO_2

There are two ways by which the electron is excited from valence band to conduction band is direct and indirect transitions by absorption of photon. According to the Tauc relation,

$$\alpha h\upsilon = B(h\upsilon - Eg)m$$

Where, B is a constant, Eg is the energy band gap, hυ is incident photon energy, m depends upon the values of electronic transitions having values 1/2, 3/2, 2 and 3. By plotting the graph between (αhυ)n vs. hυ by using n=1/m that is n=2 for direct transition, and n=1/2 for indirect, n=1/3,2/3 is for forbidden direct and forbidden indirect respectively [10].

In this case, the value of m=1/2.The absorption coefficient 'α' in the direct allowed transition may be written in the form of

$$\alpha = (h\upsilon - Eg)1/2$$

The parameters 'hυ' represents the photon energy and eg is the Energy band gap. The band gap of SnO_2 was calculated by plotting between (αhυ)1/2 vs. hυ along Y-axis and X-axis respectively. The optical band gap is found. By annealing at different temperatures, it is found that the band gap of SnO_2 is decreased due to the removal of Oxygen vacancies, where temperatures is for localizing the Oxygen atoms at the respective interstitials. The variation of the band gap with temperature is reported in the **Table 3** below [9,10,17].

Morphological Properties by SEM

Figure 5 these are the SEM images of the synthesized tin oxide or SnO_2 which has been done by the SEM (JSM-6510, SAI Labs, TIET Patiala) where it is being clearly seen the clustering of particles on the surface shows the morphology and are having fine structure, which matched with the standard structure of the SnO_2. The images are taken at three different magnification are at 0.5, 1 and 5 micrometer of the synthesized SnO_2 [18].

Elementary composition by EDX

The existence of tin particles in the tin oxide synthesized sample is been fin out by the EDS technique. The scale is from 0-14 KeV. SnO_2 which has been done by the SEM (JSM-6510, SAI Labs, TIET Patiala).

Bonding by FTIR

In order to understand the interaction of bonds in SnO_2 at various wavelengths, behavior of material at different annealing temperatures has been taken into consideration. In this regard, FTIR was used. This is confirmed by the peak at 3404.4 is due to the stretching of OH bond lying in the range 3200 and 3600 nm.

In addition, at 924.7 nm there is a bending due to Sn-OH in the range 800 to 1250 nm. And the peak at 2359.8 (C-N) is due to the carbon and nitrogen from the ammonia. The peak due to the stretching of C-O bond is at 1253.5nm [19,20].

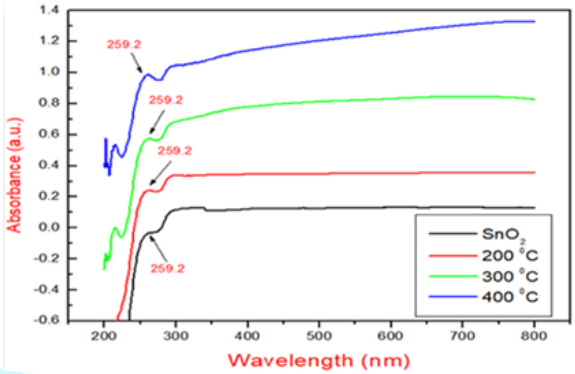

Figure 3: UV-Vis Spectra Showing the Peak values of Tin Oxide as synthesized and at various Temperatures as 200, 300, 400^{o}C.

S No.	Name	Temp. (^{0}C)	Peak Absorbance	Cut-Off Frequency	Band Gap (eV)
1	SnO_2	Synthesized	259.2 ± 2	293.2 ± 2	4.80 ± 0.1
2	SnO_2	200	259.2 ± 2	295.7 ± 2	4.60 ± 0.1
3	SnO_2	300	259.2 ± 2	303.4 ± 2	3.94 ± 0.1
4	SnO_2	400	259.2 ± 2	307.3 ± 2	3.50 ± 0.1
5	SnO_2	500	259.2 ± 2	313.3 ± 2	3.47 ± 0.1

Table 3: Showing Variation of Band Gap in SnO_2 as synthesized and at different Temperatures i.e. 200 300 400 and 500^{o}C.

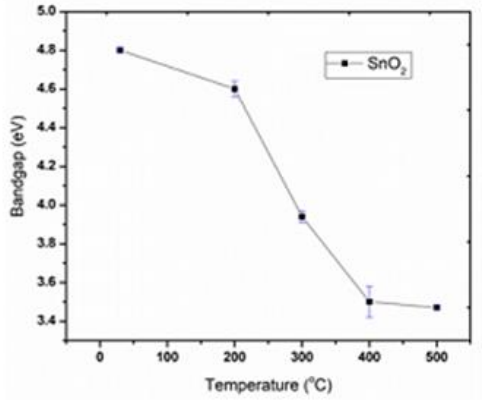

Figure 4: Variation of band gap with respect to Temperature.

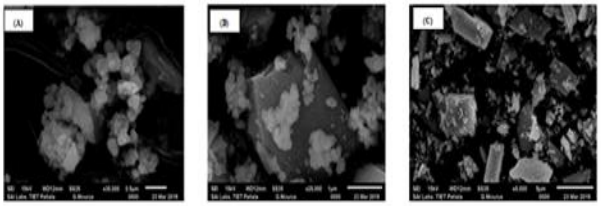

Figure 5: SEM Images of SnO2 at different magnifications at 0.5,1 and 5 micrometer in box (A), (B) and (C) respectively.

The **Figure 7** shows the FTIR of the Tin Oxide as synthesized and concealed at 400 and 500^{o}C. It has been confirmed that after calcinations at 400 and 500^{o}C. There is the broadening in the peaks which are found at 470.5 and 425.1 nm in the sample as synthesized after calcinations. Also the O-H peaks at 3404.4 and 924.7 are being removed due to the high temperature [20].

Photoluminescence

Photoluminescence is light emitted when photo-excited carriers decay from higher energy level to lower energy level. The energy of transition depends on the relative spacing of the excited and lower energy states. These states may be due to localized impurity or defect levels, continuum levels in the of electrons in conduction or valance bands, excitation states or electron-hole pairs bound by coulomb attraction, excitation states bound to impurities or defects [21,23,24].

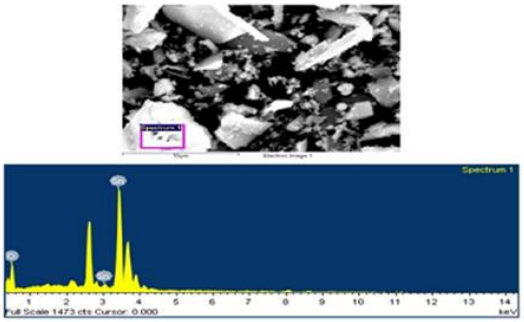

Figure 6: EDS image and plot for synthesized SnO_2 showing the Composition of the Tin and Oxygen in the material of Tin Oxide.

Functional Group	Absorption (cm-1)	Intensity
Sn-O-Sn	425.1	Strong
O-Sn-O	470.5	Strong
Sn-O	924.7	Strong
C-O	1253.5	Medium
O-H Surface	1622.7	Small
C-N	2359.8	Strong
O-H	3404.4	Strong

Table 4: List of functional groups at different Wavelengths having different intensities.

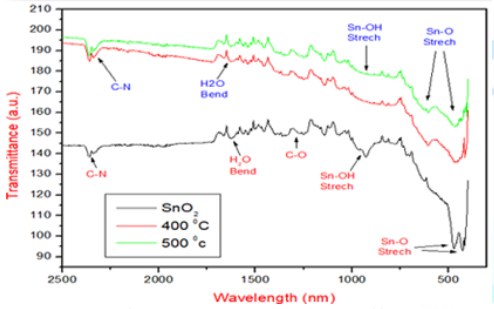

Figure 7: FTIR of Synthesized SnO_2 and at different Temperatures 400 and 500°C.

The PL spectroscopy is often used to get the information of radiative transitions among the electronic states, impurity and defects, composition of elements, energy states present in the samples. The PL emission strongly depends on structural morphological, surface area distribution and defect states. The three main emission peaks and the excitation of spectrum on tin oxide show a strong band at 375nm, 425nm and 480nm. The two main emission peaks at 375nm and 425nm (**Figure 8**) were found and till now the mechanism of observing till not yet discovered. It may be due to the defect energy levels present in the band gap of the tin oxide. We know that in oxides the Oxygen vacancies are most common defects and they act as the radiative centers in the process of luminescence [25-27,29].

In this work the synthesized tin oxide is annealed at different temperatures and all the samples were excited at 325nm as the lumincent centre. These two main peaks attributed by the electron transitions produced by defect levels present in the energy bend gap. With the increase in the temperature the bond length is reduced due to the reduction of the oxygen vacancies, hence the intensity of the emission is also reduced and the peal is shifted towards the red shift [27].

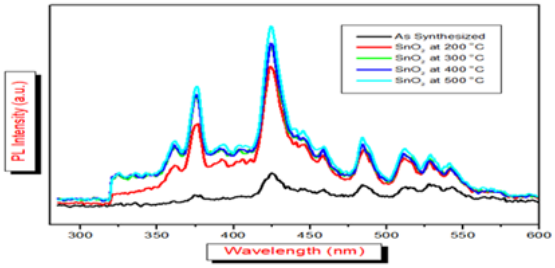

Figure 8: Pl spectra between wavelength and Intensity of SnO_2 as synthesized and SnO_2 at 200, 300 400 and 500°C.

Antibacterial Activity

From the ZONE OF INHIBITION one could see the killing efficiency of tin oxide particles is more effective on G. positive (*Micrococcus Luteus*) then G. negative *E. coli*. Hence, the tin oxide NPs exhibits the excellent antibacterial action against both the bacteria's used. We have seen the effect on the bacteria at different concentrations for both the bacteria **Figure 9**. The difference in the efficiency of tin oxide to kill or stop the growth of both the bacteria's are due to difference in the cell structure of G. positive and G. negative bacteria or chemical composition of cell of a bacteria or the chemical composition of tin oxide [28].

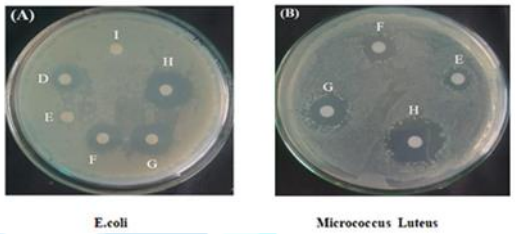

Figure 9: Showing the Effect of the SnO_2 On two different bacteria's and their zone of inhibition in the above boxes (A) and (B) *E.coli* and *Micrococcus Luteus* respectively.

Bacteria	Naming	Concentration (DMSO/1ml)	Zone of Inhibition (mm)
E. coli	E	25 mg	2
	F	50 mg	5
	G	75 mg	7
	H	100 mg	10
	I	1 mg	0
Micrococcus Luteus	E	25 mg	5
	F	50 mg	8
	G	75 mg	10
	H	100 mg	18

Table 5: Showing the zone of inhibition of SnO_2 on E. coli and *Micrococcus Luteus* on different concentrations.

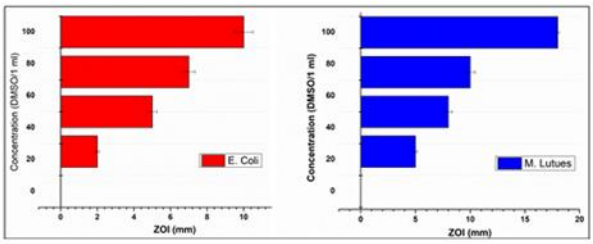

Figure 10: Comparison of antibacterial efficiency of SnO_2 nanoparticles at different concentrations between E. coli and M. luteus.

From the above results it is been clearly seen that the ZONE OF INHIBITION is directly depends upon the concentration used of the tin oxide. As we increase the concentration of tin oxide from 25-100 mg/1ml of DMSO the ZOI of both the bacteria used is increased **Table (5)**. From the above achieved results, it is clear that SnO_2 particles shows very good antibacterial activity against *Micrococcus Luteus* and comparatively less antibacterial activity against E. coli (**Figure 10**).

The difference in the behavior of tin oxide NPs towards *E Coli* and *Micrococcus Luteus* could be attributed to the fact that: the permeable nature of cell membrane of *Micrococcus Luteus* allows SnO_2 nanoparticles to penetrate and coagulate the cytoplasm of the bacteria and hence cease its activity. However, in case of *E Coli*, the presence of outer most Lipid layer which is impermeable in nature may not allow the nanoparticles to interact and hence interrupt its course of action. However, in comparison to above study, Khatoon, et al, [23] Reported that AgNPs show stronger inhibition towards gram negative bacteria than against gram positive because AgNPs may adhere on the surface of the bacteria to interact with the sulfur and phosphoric moieties of cell wall resulting in the deactivated metabolism of cell.

Conclusion

The tin oxide (SnO_2) NPs was effectively synthesized by using the Sol-gel method. The synthesized tin oxide was characterized by number of characterization which includes UV-Vis, FTIR, XRD, SEM and EDAX. It was shown that the band gap of the synthesized tin oxide was 4.80 eV, which decreases from 4.80 to 3.47 eV by increasing the temperature (200, 300, 400, and 500℃ respectively. The structural properties was studied by using XRD technique and the structure of tin oxide NPs were found as tetragonal which exactly matches with the results from JCPDS data (Card No. 88-0287). The lattice parameters were found to be equal to a=b=4.7306, c= 3.69. The average crystallite size was found in the range of 9 nm by using scherrer formula. The bonding of the various elements of tin oxide is confirmed from the FTIR technique. By using the SEM technique at different magnifications the structure of the tin oxide NPs were tetragonal. EDAX technique shows the elemental composition of tin and oxygen present in the synthesized tin oxide. At last in my paper, antibacterial activity of tin oxide which was tested on two bacteria's namely *E.coli* (Gram negative) and *Micrococcus Luteus* (Gram Positive) by zone of inhibition method. From the result the tin oxide NPs has the ability to be used as an antibacterial agent.

Acknowledgements

Asif Ahmad Bhat highly acknowledges the Institute (Lovely Professional University Phagwara) for research facility, and department of chemistry, Govt Model Degree College Shopian for their support and discussions throughout their work. M. A. Kaloo gratefully acknowledges Department of Science and Technology, New Delhi for INSPIRE-FACULTY research grants [DST/INSPIRE/04/2016/000098].

References

1. Patil GE, Kajale DD, Gaikwad VB and Jain GH. Preparation and characterization of sno2 nanoparticles by hydrothermal route (2012) Int Nano Lett 2: 17. https://doi.org/10.1186/2228-5326-2-17
2. Zhang J and Gao L. Synthesis and characterization of nanocrystalline tin oxide by sol-gel method (2004) J Solid State Chem 177: 1425-1430. https://doi.org/10.1016/j.jssc.2003.11
3. Zhu H, Yang D, Yu G, Zhang H and Yao K. A simple hydrothermal route for synthesizing SnO2 quantum dots (2006) Nanotechnology 17: 2386-2389. https://doi.org/10.1088/0957-4484/17/9/052
4. Kumar V, Singh K, Sharma J, Kumar A, Vij A et al. Zn-doped sno2 nanostructures: structural, morphological and spectroscopic properties (2017) J Mater Sci Mater Electron 28: 18849-18856. https://doi.org/10.1007/s10854-017-7836-z
5. Marton JP Jarzebski ZM. Physical Properties of SnO Materials (1976) J Electrochem Soc Rev 123: 199-205.
6. Baco S, Chik A, Yassin F and F Md Yassin. Study on optical properties of tin oxide thin film at different annealing temperature (2012) J Sci Technol 4: 61-72.
7. Adnan R, Razana NA, Rahman IA and Farrukh MA. Synthesis and characterization of high surface area tin oxide nanoparticles via the sol gel method hydrogenation styrene (2010) JCCS 57: 222-229. https://doi.org/10.1002/jccs.201000034
8. Kim H and Gilmore CM. Electrical, optical, and structural properties of indium-tin-oxide thin films for organic light-emitting devices (1999) J Appl Phys 86: 6451-6461. https://doi.org/10.1063/1.371708
9. Sanon G and Rup R. Structure Oxide (1991) phy rev 44: 5672–5680.
10. Wang J, Lu C, Liu X, Wang Y and Zhu Z, et al. Synthesis of tin oxide (SnO & SnO2) micro/nanostructures with novel distribution characteristic and superior photocatalytic performance (2017) Mat Des 115: 103-111.https://doi.org/10.1016/j.matdes.2016.11.043
11. Razeghizadeh AR, Rafee V, and Zalaghi L. Effects of changes sol concentration on the structural and optical properties of SnO2 nanoparticle by the sol-gel technique (2015) Arxiv 37: 14.
12. Ratchagar V and Jagannathan K. Synthesis and characterization of sno2 nano particles for carbon absorbing applications (2016) Orient J Chem 32: 207-212. http://dx.doi.org/10.13005/ojc/320121
13. Sagadevan S and Podder J. Investigation on structural, surface morphological and dielectric properties of zn-doped sno2 nanoparticles (2016) Mat Res 19: 420-425. https://doi.org/10.1590/1980-5373-mr-2015-0657
14. Scipioni R, Gazzoli D, Teocoli F, Palumbo O, Paolone A et al. Preparation and characterization of nanocomposite polymer membranes containing functionalized sno2 additives (2014) Membranes 4:123–142. https://doi.org/10.3390/membranes4010123
15. Nehru LC, Swaminathan V and Sanjeeviraja C. Photoluminescence studies on nanocrystalline tin oxide powder for optoelectronic devices (2012) Am J Mat Sci 2: 6-10. https://doi.org/10.5923/j.materials.20120202.02
16. Dharma J and Pisal A. Simple method of measuring the band gap energy value of tio_2 in the powder form using a uv / vis / nir spectrometer (2009) Appl. Note, 4-7.
17. Li Y, Yin W, Deng R, Chen R, Chen J et al. Realizing a Sno2-based ultraviolet light-emitting diode via breaking the dipole-forbidden rule (2012) NPG Asia Mater 4: 30. https://doi.org/10.1038/am.2012.56
18. Li R, Liu L, Ming B, Ji Y and Wang R. Oxygen vacancy effect on photoluminescence of knb3 o8 nanosheets (2018) Appl Surf Sci 439: 983-990. https://doi.org/10.1016/j.apsusc.2018.03.117
19. Khalameida S, Samsonenko M, Skubiszewska-Zięba J and Zakutevskyy O. Dyes catalytic degradation using modified tin(iv) oxide and hydroxide powders (2017) Adsorpt Sci Tech 35: 853-865. https://doi.org/10.1177/0263617417722251
20. Singh A, Ahmed B, Singh A, and Ojha AK. Photo degradation of phenanthrene catalyzed by rgo sheets and disk like structures synthesized using sugar cane juice as a reducing agent (2018) Spectrochim Acta-Part A Mol Biomol Spectrosc 204: 603-610. https://doi.org/10.1016/j.saa.2018.06.086
21. Simovic AM, Stojkovic AK, Dejan JM and Savic D. Is it possible to predict mortality in preterm neonates, based on a single troponin i value at 24 h? (2016) Ind J Pediatr 83: 466-467. https://doi.org/10.1007/s12098-015-1887-z
22. Rehman S, Asiri SM, Khan FA, Jermy BR, Khan H et al. Biocompatible tin oxide nanoparticles: synthesis, antibacterial, anticandidal and cytotoxic activities (2019) Chem Select 4: 4013-4017. https://doi.org/10.1002/slct.201803550
23. Khatoon. Antibacterial and antifungal activities of silver nanosperes synthesized by tri-sodium citrate assistedchemical approach (2017) J of environmental chem eng 148: 259-26.